



24th DAAAM International Symposium on Intelligent Manufacturing and Automation, 2013

The Wear Measurement Process of Ball Nose end Mill in the Copy Milling Operations

Vopát Tomas*, Peterka Jozef, Kováč Mario, Buranský Ivan

^a Slovak University of Technology in Bratislava, Faculty of Materials Science and Technology in Trnava, Institute of Production Technologies, Department of Machining, Forming and Assembly, Jána Bottu 25, 917 24 Trnava, Slovak Republic

Abstract

The article deals with tool wear and the cutting tool wear measurement process of ball nose end mill in the copy milling. In the experiment, we studied cutting tool wear for different types of copy milling operations. The aim was to determine and compare the wear of ball nose end mill for upward ramping and downward ramping, as well as to specify particular steps of the measurement process. In addition, we examined and observed cutter contact areas of ball nose end mill with machined material. In this article, equations for the calculation of parameters of a hemispherical milling cutter are described. The machining strategy was applied to copy milling process for mould milling. For mould milling, DMG DMU 85 monoBLOCK 5-axis CNC milling machine was used. In the experiment, the cutting tool, cutting speed and cutting feed were not changed. The cutting tool wear was measured on Zoller Genius 3s universal measuring machine. The results show different cutting tool wear depending on the copy milling strategy.

© 2014 The Authors. Published by Elsevier Ltd. Open access under [CC BY-NC-ND license](https://creativecommons.org/licenses/by-nc-nd/4.0/).
Selection and peer-review under responsibility of DAAAM International Vienna

Keywords: Cutting tool wear; ball nose end mill; ramping; effective cutting speed

1. Introduction

Ball-end milling is one of the most extensively used machining methods in manufacturing moulds and parts of sculptured surfaces, because the ball-end mill shows a reasonable spatial agreement with a sculptured surface [1]. In flat-end milling, cutting action on each cutting edge element is the same regardless of its axial position in the cutter. On the other hand, in ball end milling, cutting characteristics change along the cutting edge element due to the cutter

* Corresponding author. Tel.: 00421-904-327-267.
E-mail address: tomas.vopat@stuba.sk

geometry of the spherical part. Many researchers have proposed analytical models and explained the complex ball-end milling characteristics based on the assumption that a complex cutting process can be constructed by an aggregation of oblique cuts [2–6].

The sculptured surface machining can be classified as plain cutting, ramping, and contouring [7]. Fig. 1 shows two types of the cutter contact areas on the cutter plane for ramping. The cutter contact area always occurs in the upper half of the cutter plane during the upward ramping. In the downward ramping, the cutter contact area sometimes covers the centre of the cutter plane depending on the machining conditions [6].

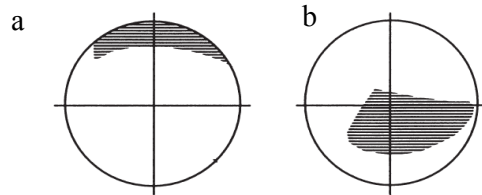


Fig. 1. (a) cutter contact area for upward ramping; (b) cutter contact area for downward ramping [6].

The sculptured surfaces are now produced on CNC milling centres enabling to produce a whole shape on one machine tool in one clamping. The most widely used are 5-axis milling centres. Parts are designed in a CAD system. Designing a part according to the application methods is important [8]. The program for CNC machine tool is generated in a CAM system [9].

In conventional machining, abrasive wear is dominant [10]. Most of the publications in the field deal with experimental analysis of the mechanism of wear in the ball nose end mill [11]. Koshy et al. [12], led a machining experimental company with hardened AISI D2 cold work tool steel (58 HRC) using a ball nose end mill to identify the tool wear mechanisms and appropriate cutting parameters, based on the analysis of flank wear patterns. They showed that chipping, adhesion and attrition mechanisms are all responsible for tool wear [12].

Schulz and Hock [13] used ball end mills with different tilt angles to study tool life and workpiece quality, and they concluded that the down-milling/reverse cut with a tool inclination in the range of 10° – 20° represents the optimum machining strategy for high-speed milling in the mould and die making industry [13].

In the experiment, we determined and compared the wear of ball nose end mill for upward ramping and downward ramping. In this article, equations for calculation of parameters of a hemispherical milling cutter are described.

2. Material and experimental methods

2.1. Tested cutting tool

Application of solid carbide ball nose end mill (specimen) is typical for mould milling. It is related to the kinematics representation of ball nose end mill in copy milling. Parameters of ball nose end mill YG-1 are shown in Table 1. The tested cutting tool material was uncoated cemented carbide. We studied two specimens (ball nose end mills), which were completely identical. Both of them were used for copy milling operations, since we investigated influence of cutter contact areas on the cutter plane on wear of ball nose end mill, which is due to the change of cutter contact area of cutting tool in copy milling operations according to upward and downward ramping. The cutting tool wear of the first specimen was examined for upward ramping (up-copying [14]) and the cutting tool wear of the other specimen was examined for downward ramping (down-copying [14]).

Table 1. Parameters of ball nose end mill.

| EDP No. | Radius of ball nose (mm) | Helix angle ($^{\circ}$) | Mill diameter (mm) | Length of cut (mm) | Number of flutes |
|----------|--------------------------|----------------------------|--------------------|--------------------|------------------|
| E5624120 | R6 | 30 | 12 | 14 | 2 |

2.2. Workpiece material

The selected workpiece material was medium-carbon steel of ISO C45 (1.0503, AISI 1045) grade. Chemical composition and mechanical properties are shown in Tables 2 and 3.

The kinematics representation of movements of ball nose end mill was implemented in machining of block material. Block material had dimensions of 100×100×60 mm. Model of workpiece was carried out in CAD system.

Table 2. Chemical composition of machined material C45.

| Element | C | Si | Mn | Ni | P | S | Cr | Mo |
|---------|----------|---------|---------|---------|-----------|-----------|---------|---------|
| wt. % | 0.43-0.5 | max 0.4 | 0.5-0.8 | max 0.4 | max 0.045 | max 0.045 | max 0.4 | max 0.1 |

Table 3. Mechanical properties of machined material C45

| Hardness (HB) | Elongation (%) | Yield strength (MPa) | Tensile strength (MPa) |
|---------------|----------------|----------------------|------------------------|
| max 225 | 16 | 340-400 | 600-800 |

2.3. Wear test

For copy milling, DMG DMU 85 monoBLOCK 5-axis CNC milling machine was used (Fig. 2a). First, the program for CNC machine tool was generated in a CAM system. Cutting fluid was not used in the machining process. As mentioned in section 2.1, we investigated two cutting tools, which were completely identical. For both cutting tests, we set the same cutting conditions (depth of cut, feed rate, and cutting speed). Hence, we intended to investigate just the influence of cutter contact areas on the cutter plane on wear of ball nose end mill for the same cutting parameters. The inclination angle of the workpiece was 15° in the ramping (Fig. 3). The cutting test of the first ball nose end mill was performed for upward ramping and the cutting test of the other ball nose end mill was performed for downward ramping.

Since the flank wear of ball nose end mill was dominant, it was measured on Zoller Genius 3s universal measuring machine (fig. 2b). The flank wear was measured every 10.75 min equivalent to 2 m length of cut. The machining tests were stopped when the flank wear reached over 0.3 mm or when catastrophic tool failure occurred.

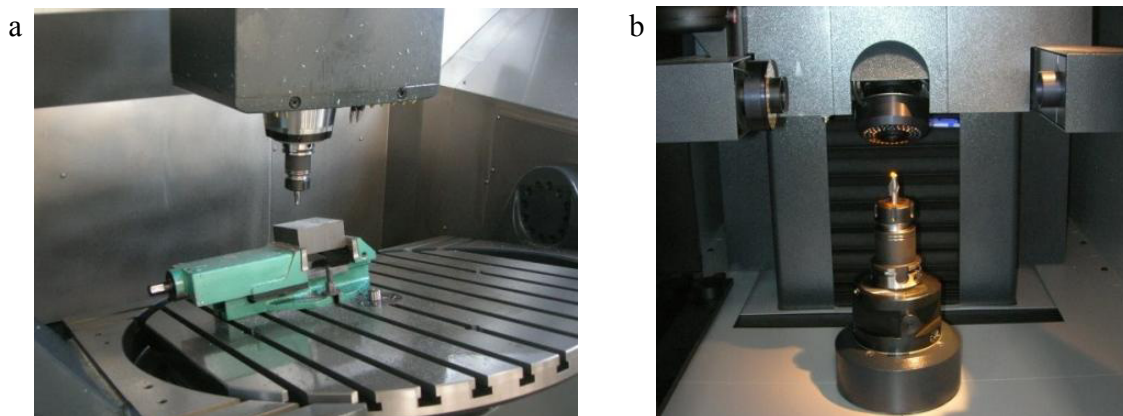


Fig. 2. (a) workplace of DMG DMU 85 mono BLOCK 5-axis CNC milling machine; (b) workplace of Zoller Genius 3s universal measuring machine.

2.4. Cutting conditions

All wear tests were carried out with the following parameters: cutting speed $v_c = 70$ m/min, frequency of spindle rotation $n = 1856.8$ 1/min, feed rate $v_f = 186$ mm/min, depth of cut $a_p = 0.5$ mm, width of cut $a_e = 0.5$ mm, feed per tooth $f_z = 0.05$ mm.

2.5. Effective cutting radius and effective cutting speed in ramping

A free form surface can be milled either by upward ramping or downward ramping. Both cases of ramping are shown in Fig. 3 [15].

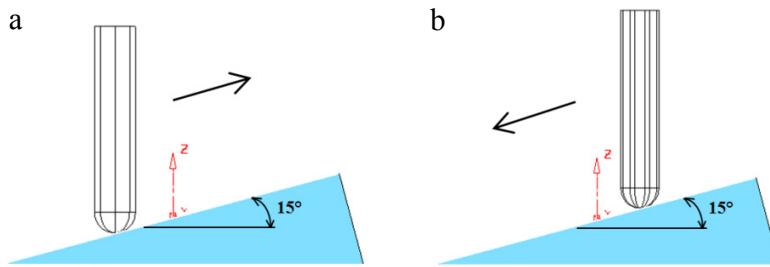


Fig. 3. (a) upward ramping; (b) downward ramping.

In the upward ramping, tangential curve is placed on the one side from the axis of rotation of ball nose end mill. In the downward ramping, tangential curve is placed around the axis of rotation of ball nose end mill on the both sides, and crosses the center of rotation of ball nose end mill. The scheme with symbols for upward and downward ramping is shown in Fig. 4. The center of rotation has not any cutting speeds. The element of cutter edge does not cut in this point.

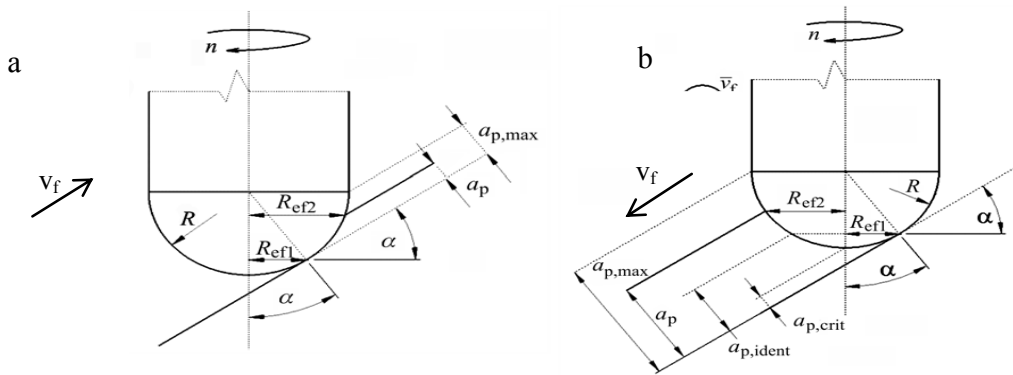


Fig. 4. (a) scheme of upward ramping; (b) scheme of downward ramping [4].

The symbols in Fig. 4:

- a_p - depth of cut (mm)
- R - radius of the cutter (mm)
- v_f - feed rate (mm/min)

α – slope angle of milling surface ($^{\circ}$)
 R_{ef1} - effective radius of the cutter on machined surface (mm)
 n - frequency of spindle rotation (1/min)
 R_{ef2} - effective radius of the cutter on work surface (mm)
 $a_{p,max}$ – maximum depth of cut (mm)
 $a_{p,iden}$ – identical depth of cut (mm)
 $a_{p,crit}$ – critical depth of cut (mm)

Specification of particular operations is determined by simultaneous movement of ball nose end mill and workpiece inclination. Tonshoff et al. [16] found that the optimum inclined angle is 15° for ball end-milling of block materials.

In technical practice, it is common that parts have different surfaces and thus various value of effective radius, which affects also the value of instantaneous effective cutting speed [4]. It is well known that the increase of cutting speed leads to increasing the flank wear. It is demonstrated in Fig. 5, where $v_{c1} > v_{c2} > v_{c3} > v_{c4} > v_{c5}$ [17].

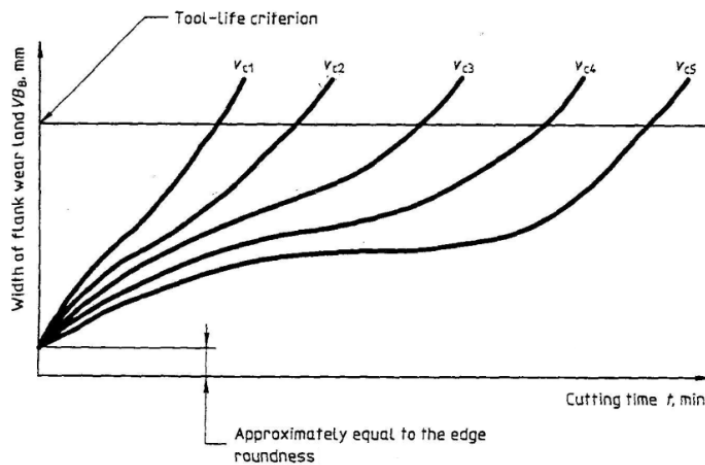


Fig. 5. flank wear progress as a function of time [17].

The importance of cutting speed can also be seen from the Taylor's equation, as the formula relies only on the cutting speed to estimate tool life (as well as tool wear). Equation 1 is also called Taylor tool-life equation [17]:

$$\begin{aligned}
 v_c \cdot T_c^{1/k} &= C \\
 T_c^{1/k} &= \frac{C}{v_c}
 \end{aligned}
 \tag{1}$$

where:

v_c – cutting speed (m/min)
 $T_c^{1/k}$ - Taylor's exponent
 C - constant.

Determination of effective radius is therefore very important for obtaining the effective cutting speed. Equations for effective radius and effective cutting speed calculation take the following forms [18]:

$$R_{ef1} = R \cdot \sin \alpha$$

$$R_{ef1} = 6 \cdot \sin 15^\circ = 1.55 \text{ mm} \quad (2)$$

$$v_{c1} = \frac{2\pi \cdot R_{ef1} \cdot n}{1000} = \frac{2\pi \cdot 1.55 \cdot 1856.8}{1000} = 18.08 \text{ m/min} \quad (3)$$

➤ The situations for upward ramping:

$$R_{ef2} = R \times \sin\left(\alpha + \arccos\frac{R - a_p}{R}\right) = R_{ef2} = 6 \times \sin\left(15 + \arccos\frac{6 - 0.5}{6}\right) = 3.74 \text{ mm} \quad (4)$$

$$v_{c2} = \frac{2\pi \cdot R_{ef2} \cdot n}{1000} = \frac{2\pi \cdot 3.74 \cdot 1856.8}{1000} = 43.63 \text{ m/min} \quad (5)$$

➤ The situations for downward ramping and provided that $a_p > a_{p,crit} \wedge a_p < R$:

$$R_{ef2} = R \times \sin\left(-\alpha + \arccos\frac{R - a_p}{R}\right)$$

$$R_{ef2} = 6 \times \sin\left(-15 + \arccos\frac{6 - 0.5}{6}\right) \quad (6)$$

$$R_{ef2} = 0.89 \text{ mm}$$

where:

R_{ef1} - effective radius of the cutter on machined surface (mm)

R_{ef2} - effective radius of the cutter on work surface (mm)

R - radius of the cutter (mm)

α - slope angle of milling surface ($^\circ$)

a_p - depth of cut (mm).

Since in downward ramping (equation 6), effective radius $R_{ef2} < R_{ef1}$, the effective cutting speed was calculated for R_{ef1} .

3. Results

3.1. The evaluation of wear test

The next step of the wear measurement process was evaluation of the wear test. First of all, the calibration process of measurement system of Zoller Genius 3 was initiated before the milling. The particular wear measurements were implemented for the first and then the second cutting edge. The average value was determined and inserted to Tables 4 and 5.

➤ upward ramping

Table 4. The measured and calculated values for upward ramping.

| No. | Time (min) | Length of cut (m) | Flank wear value VB (mm) | | Average value (mm) |
|-----|------------|-------------------|--------------------------|----------|--------------------|
| | | | 1. tooth | 2. tooth | |
| 1. | 10.750 | 2 | 0.062 | 0.072 | 0.067 |
| 2. | 21.500 | 4 | 0.111 | 0.105 | 0.108 |
| 3. | 32.250 | 6 | 0.170 | 0.137 | 0.154 |
| 4. | 43.000 | 8 | 0.229 | 0.203 | 0.216 |
| 5. | 53.750 | 10 | 0.280 | 0.247 | 0.264 |
| 6. | 64.500 | 12 | 0.302 | 0.333 | 0.318 |
| 7. | 75.250 | 14 | 0.374 | 0.333 | 0.354 |

➤ downward ramping

Table 5. The measured and calculated values for downward ramping.

| No. | Time (min) | Length of cut (m) | Flank wear value VB (mm) | | Average value (mm) |
|-----|------------|-------------------|--------------------------|----------|--------------------|
| | | | 1. tooth | 2. tooth | |
| 1. | 10.750 | 2 | 0.070 | 0.070 | 0.070 |
| 2. | 21.500 | 4 | 0.100 | 0.103 | 0.102 |
| 3. | 32.250 | 6 | 0.140 | 0.134 | 0.137 |
| 4. | 43.000 | 8 | 0.178 | 0.162 | 0.170 |
| 5. | 53.750 | 10 | 0.220 | 0.197 | 0.209 |
| 6. | 64.500 | 12 | 0.264 | 0.231 | 0.248 |
| 7. | 75.250 | 14 | 0.298 | 0.283 | 0.291 |
| 8. | 86.000 | 16 | 0.344 | 0.316 | 0.330 |

Flank wear values for upward ramping are described in Table 4 and for downward ramping in Table 5. As written in section 2.3, we measured flank wear and inserted the flank wear values to the tables after every 10.75 min (equivalent to 2 m length of cut). In upward ramping, the flank wear value reached over 0.3 mm after 64.5 min of cutting. As can be seen in measurement No. 8 (Table 4), the flank wear value on the second tooth is same as the flank wear value in measurement No. 7. It is caused by the chipping of cutting edge. The flank wear increased, but chipping of cutting edge caused that the measured value of flank wear decreased due to the chipping. In downward ramping, the flank wear value reached over 0.3 mm after 86 min of cutting.

The graph in Fig. 6 plotted based on flank wear value of particular measurement expresses the time dependence of flank wear. The time dependence of flank wear for upward and downward ramping was then compared.

As can be seen in Fig. 6, the flank wear of ball nose end mill in downward ramping is smaller than in upward ramping. We suppose that it is due to two factors. Factor 1 is that effective cutting speed for upward ramping is 2.41 times greater than for downward ramping. As explained in sections 2.5, increase of cutting speed leads to the increase of flank wear. Factor 2 may be that the cutter contact area was greater in downward ramping.

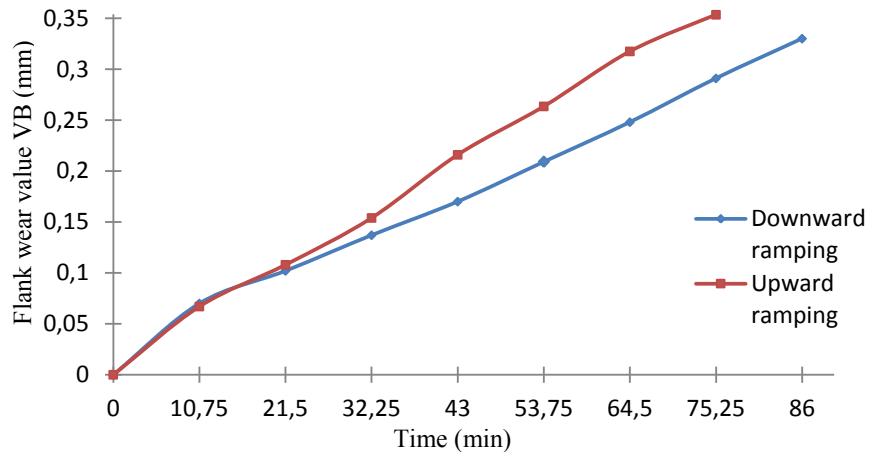
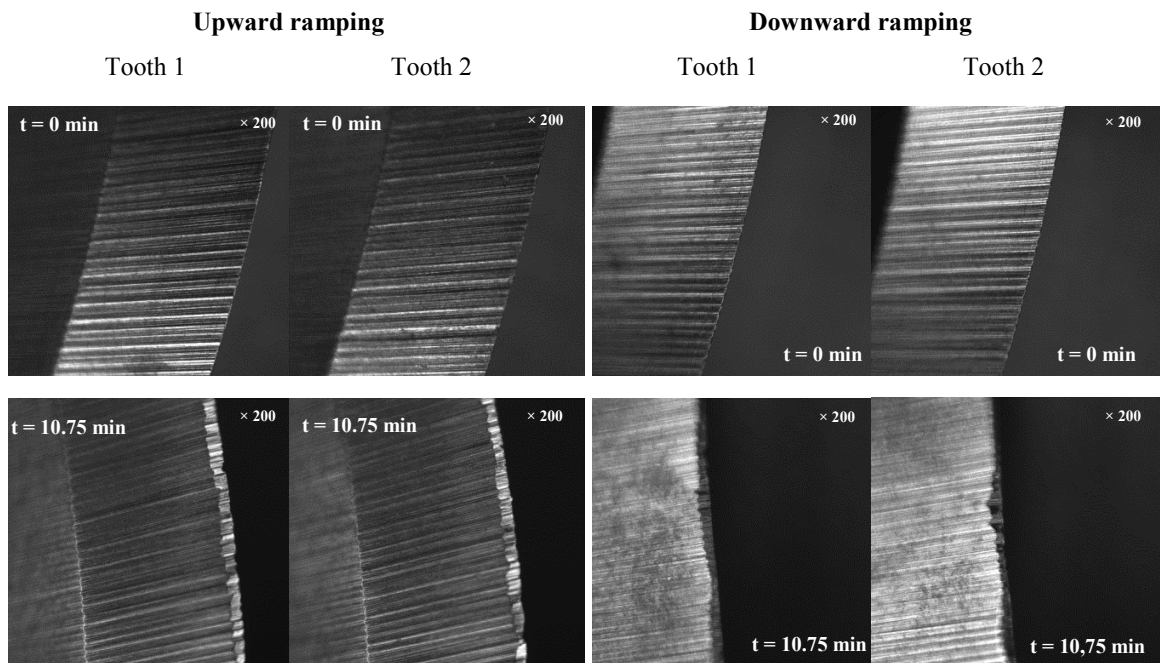


Fig. 6. the time dependence of flank wear.

3.2. Measured flank wear in micrographs

The measured flank wear is shown in Fig. 7. The first two columns are micrographs of flank wear for upward ramping. The other two columns are micrographs of flank wear for downward ramping. Fig. 7 records flank wear of ball nose end mill before cutting in time of 0 min and after the first measurement in time of 10.75 min. Furthermore, the last two lines show measured flank wear before attaining the value of 0.3 mm (in time of 53.75 min for upward ramping and in time of 75.25 for downward ramping) and after attaining the value of 0.3 mm (in time of 64.5 min for upward ramping and in time of 86 min for downward ramping).



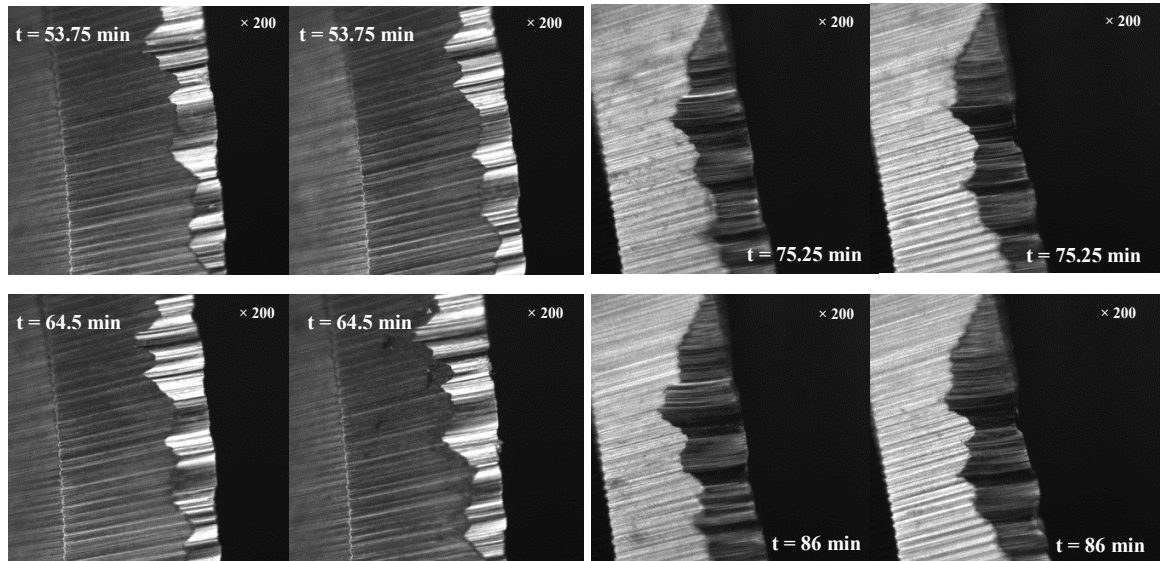


Fig. 7. Micrographs of flank wear.

4. Conclusion

The aim was to determine the wear of ball nose end mill in dependence of selected strategy of ramping. The tool wear criterion was the flank wear value, because it was dominant. In the experiment, we determined and compared the wear of solid carbide ball nose end mill for upward and downward ramping.

We investigated two cutting tools, which were completely identical. For both cutting tests, we set the same cutting conditions (depth of cut, feed rate, and cutting speed). Then, we investigated influence of cutter contact areas on the cutter plane on wear of ball nose end mill for the same cutting parameters. The cutting test of the first ball nose end mill was performed for upward ramping, and cutting test of the second ball nose end mill was performed for downward ramping. The worn cutter contact areas of ball nose end mill was first calculated and then observed on Zoller Genius 3s universal measuring machine. For wear test, DMG DMU 85 monoBLOCK 5-axis CNC milling machine was used. The cutting tool wear was measured on Zoller Genius 3s universal measuring machine.

The results showed different flank wear according to the copy milling strategy. We measured flank wear every 10.75 min (equivalent to 2 m length of cut) particularly for upward and downward ramping. In upward ramping, the flank wear value reached over 0.3 mm after 64.5 min of cutting. In downward ramping, the flank wear value reached over 0.3 mm after 86 min of cutting. The flank wear of ball nose end mill in downward ramping is smaller than in upward ramping. We suppose that it is caused by two factors:

- Factor 1: effective cutting speed for upward ramping is 2.41 times greater than for downward ramping. As explained in section 2.5, the increase of cutting speed leads to the increase of flank wear;
- Factor 2: cutter contact area was greater in downward ramping.

The study results show that the tool life of ball nose end mill is longer in downward ramping. Hence, selection of downward ramping operation is preferable for copy milling for the case mould milling, when the cutting tool wear is the main criterion. The future study will be complemented by other cutting tool materials (such as high speed steel) and also coated cutting tools. In addition, further research will be completed by longitudinal upward and longitudinal downward ramping.

Acknowledgements

This contribution is a part of the GA VEGA project of Ministry of Education, Science, Research and Sport of the Slovak Republic, No. 1/0615/12 “Influence of 5-axis grinding parameters for geometric precision of cutting shank tool”.

This contribution is also supported by the Operational Project Research and Development of Centre of Excellence of five axis machining, ITMS 26220120013, co-financed by European Funds for Regional Development.

*This contribution is elaborated by support
of Operational Project Research and Development
of Centre of Excellence of Five Axis Machining,
ITMS 26220120013, co-financed
by European Funds for Regional Development.*



We are supporting research activities in Slovakia/
Project is co-financed by sources of ES

References

- [1] G.M. Kim, B.H. Kim, C.N. Chu, Estimation of cutter deflection and form error in ball-end milling processes. *International Journal of Machine Tools & Manufacture* 2003; 43 pp. 917–924.
- [2]] M.Y. Yang, H.D. Park, The prediction of cutting force in ball-end milling, *Int. J. Mach. Tools Manufact.* 31 (1991) pp. 45–54.
- [3] C. Sim, M.Y. Yang, The prediction of the cutting force in ball-end milling with a flexible cutter, *Int. J. Mach. Tools Manufact.* 33 (1993) pp. 267–284.
- [4] C.C. Tai, K.H. Fhu, A predictive force model in ball-end milling including eccentricity effects, *Int. J. Mach. Tools Manufact.* 34 (1994) pp. 959–979.
- [5] C.C. Tai, K.H. Fhu. Model for cutting forces prediction in ball-end milling, *Int. J. Mach. Tools Manufact.* 35 (1995) pp. 511–534.
- [6] G.M. Kim, P.J. Cho, C.N. Chu, Cutting force prediction of sculptured surface ball-end milling using Z-map, *Int. J. Mach. Tools Manufact.* 40 (2000) pp. 277–296.
- [7] C.N. Chu, S.Y. Kim, J.M. Lee, Feed-rate optimization of ball end milling considering local shape features, *Annals of the CIRP* 46 (1997) pp. 433–436.
- [8] J. Jurko, M. Ďzupon, A. Panda et al, Deformation of material under the machined surface in the manufacture of drilling holes austenitic stainless steel. *Chemické listy*, 105, (S)(2011), pp. 600-60.
- [9] P. Pokorný, J. Peterka, Š. Václav, The task of 5-axis milling. *Tehnicki Vjesnik - Technical Gazette*. Vol. 19, No. 1 (2012), pp. 147-150 ISSN 1330-3651.
- [10] M. Sokovića, J. Kopača, L.A. Dobrzańskib et al, Wear of PVD-coated solid carbide end mills in dry high-speed cutting, *Journal of Materials Processing Technology*, vol. 157-158 (2004) pp. 422–426.
- [11] M. Ben Said, K. Saï, W. Bouzid Saï, An investigation of cutting forces in machining with worn ball-end mill, *Journal of Materials Processing Technology* 209 (2009), pp. 3198–3217.
- [12] P. Koshy, R.C. Dewes, D.K. Aspinwall, High speed end milling of hardened AISI D2 tool steel (58 HRC), *Journal of Materials Processing Technology* 127 (2002), pp. 266–273.
- [13] H. Schulz, S. Hock, High-speed milling of die and moulds – cutting conditions and technology. *Annals of the CIRP* 44 (1995) pp. 35-38.
- [14] Sandvik Coromant. Contouring or copy milling. http://www.sandvik.coromant.com/en-gb/knowledge/milling/application_overview/profile_milling/contouring_or_copy_milling/pages/default.aspx
- [15] P. Pokorný, Technological factors of CNC milling of free form surfaces. Habilitation thesis, Trnava, STU in Bratislava, 2009, p. 94.
- [16] H.K. Tonshoff, J. Hernandez-Camacho, Die manufacturing by 5 and 3 axes milling, *Journal of Mechanical Working Technology* 20 (1989) pp. 105-119.
- [17] International Organization for Standardization. Tool-life testing with single-point turning tools, 1993. ISO 3685.
- [18] J. Peterka, Analysis of the geometry and kinematics of copy milling, in *Vedecké práce (Science Theses) MTF STU in Trnava*, 5, 1997, pp. 53- 58.